Radiation Measurements 47 (2012) 492–500

Contents lists available at SciVerse ScienceDirect

Radiation Measurements

journal homepage: www.elsevier.com/locate/radmeas

Monte Carlo modelling for the *in vivo* lung monitoring of enriched uranium: Results of an international comparison

D. Broggio [a,*], J. Bento [b], M. Caldeira [b], E. Cardenas-Mendez [c], J. Farah [a], T. Fonseca [d], C. Konvalinka [e], L. Liu [f], B. Perez [g], K. Capello [c], P. Cowan [h], J.-A. Cruzate [i], L. Freire [j], J.-M. Gómez-Ros [g], S. Gossio [i], B. Heide [k], J. Huikari [l], J. Hunt [m], S. Kinase [n], G.H. Kramer [c], O. Kurihara [o], A. Kyrieleis [h], A.-L. Lebacq [d], D. Leone [k], C. Li [f], J. Li [f], L.-C. Mihailescu [d], M. Moraleda [g], J.-F. Navarro [g], C. Oliveira [b], N. Puerta [i], U. Reichelt [e], C. Simões [b], D. Sommer [e], M. Takahashi [n], P. Teles [b], F. Vanhavere [d], T. Vrba [p], D. Franck [a], G. Gualdrini [q], M.-A. Lopez [g]

[a] *Institut de Radioprotection et de Sûreté Nucléaire, IRSN/DRPH/SDI/LEDI, BP-17, F92262 Fontenay-aux-Roses, France*
[b] *Instituto Tecnológico e Nuclear, Estrada Nacional 10, 2686-953 Sacavém, Portugal*
[c] *Human Monitoring Laboratory, 775 Brookfield Road, PL6302D, Ottawa, Ontario K1A 1C1, Canada*
[d] *SCK-CEN, Boeretang 200, 2400 Mol, Belgium*
[e] *Technische Universität Dresden, Helmholtzstraße 10, 01069 Dresden, Germany*
[f] *Laboratory of Radiation Protection and Environmental Protection, Department of Engineering Physics, Tsinghua University, Beijing 100084, China*
[g] *CIEMAT, Avd. Complutense 22, 28040 Madrid, Spain*
[h] *Serco, Thomson House, Birchwood Park, Warrington/Cheshire WA3 6GA, UK*
[i] *Autoridad Regulatoria Nuclear, Av. Libertador 8250, Buenos Aires, Argentina*
[j] *Escola Superior de Tecnologia da Saúde de Lisboa, Av. D. João II, Lote 4.69.01, 1990 - 096 Lisboa, Portugal*
[k] *Institut fuer Nukleare Entsorgung - Karlsruher Institut fuer Technologie, Hermann-von-Helmholtz-Platz 1, 76344 Eggenstein-Leopoldshafen, Germany*
[l] *Säteilyturvakeskus (STUK), Laippatie 4, FI-00881 Helsinki, Finland*
[m] *IRD - Instituto de Radioproteção e Dosimetria, Av. Salvador Allende s/n –Jacarepaguá, Rio de Janeiro, CEP - 22780-160, Brazil*
[n] *Japan Atomic Energy Agency, Tokai-mura, Naka-gun, Ibaraki-ken 319-1195, Japan*
[o] *Japan Atomic Energy Agency, Nuclear Fuel Cycle Engineering Laboratories, 4-33 Muramatsu, Tokai-mura, Ibaraki 319-1194, Japan*
[p] *CTU in Prague, Faculty of Nuclear Sciences and Physical Engineering, FNSPE, Brehova 7, 11519 Praha, Czech Republic*
[q] *ENEA Radiation Protection Institute, Via dei Colli 16, 40136 Bologna, Italy*

HIGHLIGHTS

- We perform well-defined *in vivo* calibration measurements of enriched uranium in lungs.
- A voxel model of the phantom and other needed data are provided to participants.
- Participants perform Monte Carlo simulation of the counting efficiencies.
- For about half of the participants the agreement with experiment is within ±5%.
- Other participants needed support to obtain this agreement.

ARTICLE INFO

Article history:
Received 21 October 2011
Received in revised form
16 February 2012
Accepted 24 April 2012

Keywords:
In vivo measurements
Monte Carlo computation
Internal dosimetry
Worker monitoring
Intercomparison

ABSTRACT

In order to assess the reliability of Monte Carlo (MC)-based numerical calibration of *in vivo* counting systems the EURADOS network supported a comparison of MC simulation of well-defined experiments. This action also provided training for the use of voxel phantoms. *In vivo* measurements of enriched uranium in a thoracic phantom have been carried out and the needed information to simulate these measurements was distributed to 17 participants. About half of the participants managed to simulate the measured counting efficiency without support from the organisers. Following additional support all participants managed to simulate the counting efficiencies within a typical agreement of ±5% with experiment.

* Corresponding author.
E-mail address: david.broggio@irsn.fr (D. Broggio).

1350-4487/$ – see front matter © 2012 Elsevier Ltd. All rights reserved.
doi:10.1016/j.radmeas.2012.04.020

1. Introduction

In vivo monitoring consists of measuring the radiations emitted from the body using specialised counting systems, mainly NaI(Tl) or germanium detectors, in order to assess the activity in the body or in an organ. *In vivo* monitoring is performed periodically for the routine monitoring of nuclear workers or occasionally when an incidental incorporation of radionuclides is suspected. To calibrate the counting systems, specific physical phantoms containing radioactive sources and representing the human body, or parts of it, are used. The use of calibration phantoms allows the count rate measured during the monitoring to be converted into retained activity that enables the assessment of dose (ICRP, 1997; ICRU, 2003).

However, the available physical phantoms are far from representing all the possible human body type; the distribution of activity in these phantoms is also fixed and it can be significantly different from the distribution predicted by the biokinetic modelling of radionuclides (Lamart et al., 2009). For these reasons, and others, efforts have been undertaken to develop numerical methods for calibrating *in vivo* counting systems (Hunt et al., 1998; Franck et al., 2001). For this purpose, numerical models of the human body are built, the counting system is modelled and calibration factors are obtained using Monte Carlo (MC) calculations. To assess the reliability of such calculations it must be verified that well-defined counting experiments can be simulated.

Although several teams have used such calibration methods for different cases (Hunt et al., 1999; de Carlan et al., 2003; Broggio et al., 2009; Malátová et al., 2010) their use is still quite limited. In order to assess the reliability of MC *in vivo* modelling, the Eurados network already recently supported a comparison of calculated counting efficiency in the case of a knee phantom contaminated with ^{241}Am (Gómez-Ros et al., 2007, 2008a,b). Due to the interest of participants for this comparison, and in order to provide training, a similar action was conducted about the MC modelling of enriched uranium *in vivo* lung monitoring. This project was supported by the working group 6 “computational dosimetry” (Lopez et al., 2011) and 7 “internal dosimetry” of the Eurados network.

Reference measurements have been carried out with the Livermore phantom and germanium detectors of the CIEMAT *in vivo* counting unit. Voxel phantoms of the Livermore phantom and reference data such as the counting positions, activity of the sources, etc were provided to the participants. Participants were asked to compute the spectra measured by the detectors and to give the counting efficiencies for energies of interest. A first round of analysis was carried out and when the disagreement with experimental quantities was larger than expected, as assessed by the organisers' MC simulations, participants were asked to review their results. For this purpose tutorials were distributed and personal advice given when appropriate.

This paper details the preparation of reference data and measurement, reports on the final agreement of calculated and experimental quantities and analyses the main source of errors and ambiguities that can lead to disagreement by orders of magnitude between experimental and calculated quantities.

2. Materials and methods

2.1. Experimental measurements

The measurements were carried out at the CIEMAT *in vivo* counting unit (Lopez Ponte and Bravo, 2000). The detection system consisted of two pairs of Canberra low energy germanium detectors (LE Ge) mounted in an ACTII cryostat. Each detector contains a germanium crystal 25-mm thick and 70 mm in diameter and the entrance window is made of carbon fibre and epoxy resin. Reference spectra acquired during the experiments hereafter described are the sum of spectra of each individual detector.

A first measurement was made with a ^{241}Am point source (activity 38.4 kBq) located below the detectors and at about an equal distance of the four detectors. The positions of the source and of the detectors centres were measured on a reference frame designed for this experiment. The accuracy for the measured position of the source and detectors was estimated to be ± 3 mm.

Two measurements were then carried out using the Livermore phantom (Griffith et al., 1978) with lungs containing enriched uranium. The activity of uranium isotopes in each lung, as given by the manufacturer is shown in Table 1, the uncertainty for the activities is 5% ($k = 1$). For the first measurement (P0 measurement) the Livermore phantom was not equipped with an extra-thoracic plate; for the second one (P4 measurement) it was equipped with the biggest extra-thoracic plate (thickness 24 mm). These plates are used to obtain calibration factors corresponding to individuals of increasing chest-wall thickness. These plates are made of tissue equivalent materials simulating the absorption of a mixture of muscle and adipose tissue (Kramer and Hauck, 2002). The Livermore phantom was positioned on a reference frame made out of a large sheet of graph paper. The uncertainty for the measured positions of the detectors on this frame is the same as that for the point source experiment. The frame and the Livermore phantom were marked so that the phantom could be positioned in a reproducible manner on the frame. For the P0 measurement the counting time was 2 h, it was 5 h for the P4 measurements. After the measurements the spectra were analysed with the Abacos software[1] (Canberra company). The variation of the full width at half maximum (FWHM) of photopeaks with energy was fitted and recorded. The positioning of the detectors did not provide an optimum counting efficiency since the detectors were not covering the lungs as well as in routine measurements. However, the selected positioning allowed the detectors to remain vertical and enabled a more accurate measurement and simulation of detectors' positions than in the routine practice. The detectors, Livermore phantom and reference frame are shown in Fig. 3 (Section 3.3).

2.2. Voxel phantoms construction

CT scans of the Livermore phantoms were used to build voxel phantoms corresponding to the P0 and P4 cases. For this purpose, the left and right lungs, the bones, whole body and P4 plates were delineated with the Isogray Treatment Planning System (Isambert et al., 2007; Dosisoft, 2010). Isogray performs a mesh based 3D reconstruction of delineated organs; the mesh data were provided to the binvox[2] utility so that a voxel phantom was obtained. More details about a similar construction method are given in (Farah et al., 2011). Since the dimensions of the voxel model slightly disagreed with the measured dimensions of the physical phantom, a few voxel planes were added in the transverse and coronal directions so that the dimensions were finally equal.

The main characteristics of the P0 and P4 voxel phantoms are given in Table 2. For both phantoms the voxels are cubic and have a volume of 8 mm^3, for the P4 case the total number of voxels is about 9×10^6. As shown in Table 2 the obtained volume for lungs is not exactly the same for both voxel phantoms but the difference is small enough to be disregarded. The differences in volumes are

[1] http://www.canberra.com/fr/pdf/produits/HP/ABACOS.pdf (accessed February 2012).

[2] http://www.cs.princeton.edu/~min/binvox/ (accessed February 2012).

Table 1
Activities of uranium isotopes for the lung sources.

	Left lung activity (Bq)	Right lung activity (Bq)
^{234}U	17,750	24,500
^{235}U	677.6	935.4
^{238}U	3401	4696

attributed to the differences in the contouring of the two sets of CT scan images (one image set for P0 and one for P4).

2.3. Requested simulation tasks and data provided to participants

The project was divided into three tasks but it was not mandatory for participants to take part in all of them.

The *first task* consisted of modelling the ^{241}Am point source measurement. Participants were asked to compute the pulse height spectrum between 7 and 64 keV using 214 energy bins, which corresponds to the experimental conditions. They were then asked to compute the counting efficiency for the 59.5 keV photopeak using the same region of interest than for the measurement. The requested units were counts/s for the spectrum and counts/s/Bq for the efficiency. A similar task was specified in the previous intercomparison exercise (Gómez-Ros et al., 2007, 2008a,b) and it can be seen as a preparation for the second task since it helps in implementing the detector model in MC codes.

The *second task* consisted of modelling the P0 and P4 measurements. Participants were asked to compute the pulse height spectrum between 31 and 210.5 keV over 672 energy bins, the energy per channel being equal to the experimental one. They were then asked to compute the counting efficiency at 63.3, 143.8 and 185.7 keV. The first photopeak is due to ^{234}Th and is used to assess the activity of ^{238}U, the two other photopeaks are due to ^{235}U and thus enable direct assessment of its activity. The requested units for the spectra and efficiencies were the same as that for task 1. Regions of interest, slightly different for the P0 and P4 cases (but as used in the experimental assessment of counting efficiency) were provided to compute efficiencies. Specifically, the participants were asked to detail the method to compute efficiency; particularly it was asked if the computed efficiencies were obtained from the simulated spectra. Indeed, with MC calculations it is not necessary to simulate all the details of the spectrum to obtain the counting efficiency at a given energy, for instance one can simulate only the requested energy in the source to save computing time or obtain better statistics. For the two tasks only the sum spectrum of the four detectors was requested.

The *third task* can be seen as an extra task. Participants were asked to carry out their own lung *in vivo* measurements and try to simulate them, participants were invited to contact the CIEMAT *in vivo* counting unit to schedule measurements or to carry out measurements in their own facility. This third task was intended to demonstrate one of the main difficulties in simulating *in vivo* counting experiments: reproducing in the simulation the relative positioning of detectors and measured subjects.

2.4. Data provided to participants

The information provided to participants consisted of a single text explaining the requested tasks and providing technical data[3]. It also consisted of the voxel phantom data that were provided separately.

Table 2
Characteristics of the voxel phantoms provided to participants.

	P0 voxel phantom	P4 voxel phantom
Voxel phantom dimensions (number of voxels)	255 × 239 × 139	255 × 239 × 148
Left lung volume (L)	1.76	1.72
Right lung volume (L)	2.39	2.36
Body tissue volume (L)	27.54	27.62
Extra-thoracic plate volume (L)	–	4.73
Bone volume (L)	1.54	1.52

The voxel phantoms were distributed in two formats. The first format was a single binary file containing the 3D matrix representing the phantom. The second format was a collection of ASCII files, each one defining the nature of voxels in the axial planes of the voxel model.

In the text explaining the requested tasks, apart from data described above the following information were available:

- definition of counting efficiency and indications on how to calculate it from a spectrum;
- the energy-dependent equation defining the FWHM of photopeaks;
- instructions on how to read and use the voxel phantoms;
- technical drawing of the detectors with associated materials, as already used in the previous exercise;
- technical drawing of the point source with associated materials' definition;
- definition of the materials for the voxel models, the material composition was assessed at best from a literature study (Griffith et al., 1978; Newton and White, 1978; Kramer and Hauck, 2002), data provided by the manufacturer, and preceding experience in simulation with the Livermore phantom (Pierrat, 2005).
- exact definition of the counting positions, given in a reference frame whose origin was a corner of the voxel phantom;
- values for the energy and yields of gamma ray of ^{234,235}U, ^{230,231,234}Th, ^{234m}Pa, ^{241}Am, compiled and selected from different reference tables (Browne and Firestone, 1986; ICRP, 1983; ICRP, 2008).

The material specification for the Livermore voxel models is reproduced in Table 3.

2.5. Analysis of results

The organisers had performed the requested tasks and checked that their simulations were in a good agreement with the experimental results; it was thus expected that the agreement between efficiencies calculated by participants and the experimental

Table 3
Composition (in weight percent) and density recommended for the definition of voxel phantoms' materials.

	Lungs	Body tissue	P4 plate	Bones	Air
H	8	9.03	9.24	6.38	
C	60.8	59.37	60.73	47.2	
N	4.2	3.3	3.85	2.12	75.5
O	24.9	26.6	25.4	31.3	23.2
Ar					1.3
Ca	2.1	1.7	0.78	13	
Density (g/cm^3)	0.26	1.06	1.06	1.26	1.205×10^{-3}

[3] The text is available on the Eurados web site (http://www.eurados.org/), in the menu "actions" and sub-menu "intercomparisons" (accessed February 2012). All data can be also obtained upon request to the corresponding author.

efficiencies would have similar agreement. The analysis of results for task 1 and 2 is based on the same method. Results of participants were classified as accepted or requiring revision.

If a reasonable agreement (~20%) was obtained for the efficiencies it was checked that the provided spectra were correct (in order to be sure that the provided efficiencies were not correct due to compensating errors) and the results were classified as accepted.

When several or all of the calculated efficiencies were in clear disagreement with experimental values (disagreement typically larger than ±50%) the results were classified as demanding revisions. Some participants obtained efficiencies that seemed correct but the organisers identified that the calculation from the computed spectra could be improved, these results were also classified as requiring revision. Finally, some results were classified as requiring revision because the reported efficiencies were wrong due to inattention errors (i.e. efficiencies for the P4 case attributed to the P0 case, etc).

For results requiring revision, additional data were provided to participants. The first one consisted of a spreadsheet tutorial showing how to compute efficiency from a spectrum. The second one consisted of a personalised report. In this report one of the participant's spectra and a corresponding reference computational spectrum were plotted. Since in most cases there was only a scaling factor between the two spectra, this scaling factor was indicated in the report and it was asked to study the error leading to the scaling factor. In this report, the participant's method to compute the efficiency from a spectrum was also analysed and when it did not follow the expected method, the method provided in the tutorial.

In some cases both the spectra and the efficiency calculation method were incorrect; however, the organisers were able to trace the exact source of the error in most cases but it was not reported to the participants.

3. Results and discussion

3.1. Statistics about participants and used MC codes

Seventeen teams took part in this comparison initiative; it represented 14 institutes or companies since in 3 institutes two independent teams took part in the exercise. The 14 institutes are listed in the authors' affiliation. The ENEA did not participate but provided support for the organisation of this project. Since it was not mandatory to participate in all tasks, 15 answers were received for task 1 and 16 answers were received for task 2. For task 3, only two teams accepted to carry out their own experiment at CIEMAT and only one participant reported data from experiments carried out in his facility. As a result, only tasks 1 and 2 are discussed in this paper. To preserve anonymity each participant is hereafter defined by a letter (A to Q), which will be used in reporting the results.

Eleven participants used the MCNPX code (Pelowitz, 2005), other used codes were MCNP (Briesmeister, 1997), AMOS (Gabler et al., 2006), EGS4 in conjunction with the UCWBC code (Nelson et al., 1985; Kinase et al., 2007), MCBEND (Cowan et al., 2009), PENELOPE (Baró et al., 1995) and VMC (Hunt et al., 2003). MC codes are listed with the anonymous ID of participants in Table 4.

3.2. Point source experiment simulation (task 1)

From the 15 answers received for task 1, 8 were accepted and 7 needed revision. For the accepted results the agreement between experimental and computed efficiencies was within 3%. From the seven results needing revision it was concluded that for six of them the spectra were correct but the efficiency calculation was wrong, nevertheless this difficulty in calculating the efficiency lead to answers between 7.1×10^{-3} and 2.3×10^{-2} (supposed to be counts/s/Bq). For the last answer needing revision a scaling factor between the expected spectrum and the computed one was identified.

Table 4
Monte Carlo codes used by participants.

Participant ID	Used code	Participant ID	Used code
A	MCNPX 2.7a	J	MCNPX 2.6f
B	MCNPX 2.5–2.6	K	EGS4
C	MCNPX 2.7b	L	MCNP4c
D	MCNPX 2.5f	M	MCNPX 2.7b
E	MCNPX 2.6	N	MCBEND 10A
F	MCNPX 2.6d	O	MCNPX 2.6
G	PENELOPE	P	AMOS
H	MCNPX 2.6c	Q	MCNPX 2.6c
I	VMC		

The accepted and corrected results, for efficiency at 59.5 keV, are shown in Table 5. Except for two participants, the agreement with the experimental efficiency is within 3%. In most cases the computed efficiency is higher than the experimental one.

A selection of computed spectra is compared with the experimental spectrum (normalised to 1 s counting time) in Fig. 1 where it can be seen that the 59.5 keV photopeak, Compton profile and back-scattered part of the spectrum are simulated with a good precision. As already discussed elsewhere (Ménard, 2004) the low-energy part of the spectrum is more difficult to simulate, this is probably mainly due to the transport of low-energy electrons and photons but also inaccuracy of material composition definition. Furthermore X-rays consist of several lines that were not simulated separately. Obtaining a better agreement for this part of the spectrum would require additional studies, which is not the purpose of the work presented here.

3.3. In vivo measurements simulation (task 2)

From the 16 answers received, 7 were accepted and 9 needed revisions. For the nine cases needing revisions, it was considered that in three cases the revisions were minor (misprint in reported results or slight improvement of the efficiency calculation needed). In the P0 case the experimental efficiency at 63.3 keV was 3.25×10^{-4} counts/s/Bq, before correction of results the received answers ranged between 1.3×10^{-6} and 7.9×10^{-1}. These values

Table 5
Comparison of experimental and simulated counting efficiencies for task 1 (modelling of 241Am point source counting).

Participant ID	Status	Efficiency @ 59.5 keV (counts/s/Bq)	Difference with experiment [%]
Experiment	–	8.13×10^{-3}	–
A	Corr.	6.72×10^{-3}	17.3
B	Acc.	8.35×10^{-3}	2.7
C	Corr.	8.20×10^{-3}	0.9
D	Acc.	8.21×10^{-3}	1.0
E	Corr.	8.16×10^{-3}	0.4
F	Corr.	8.64×10^{-3}	6.3
G	Acc.	8.27×10^{-3}	1.7
H	Acc.	8.30×10^{-3}	2.1
I	–	–	–
J	Corr.	7.90×10^{-3}	2.8
K	–	–	–
L	Acc.	8.25×10^{-3}	1.5
M	Corr.	8.26×10^{-3}	1.6
N	Corr.	8.24×10^{-3}	1.4
O	Acc.	8.34×10^{-3}	2.6
P	Corr.	8.38×10^{-3}	3.1
Q	Acc.	8.25×10^{-3}	1.5

The status "Acc." means that submitted results did not required corrections ("Corr."). Participants I and K only took part in task 2.

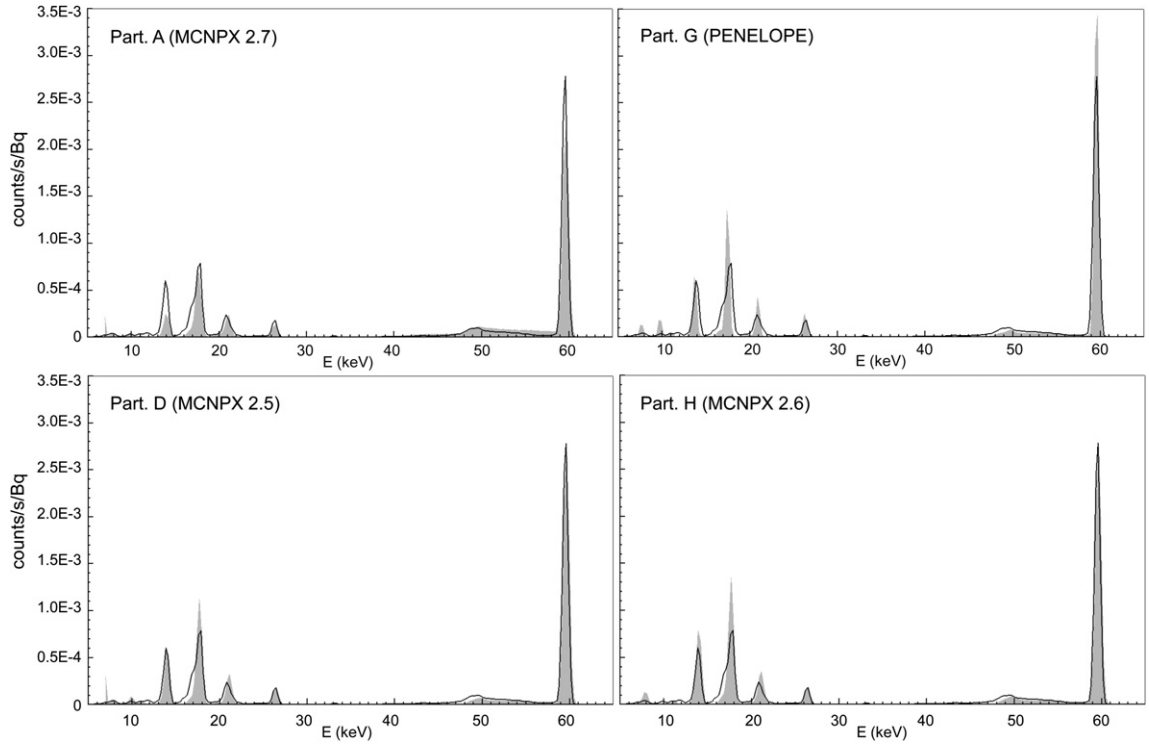

Fig. 1. Comparison of experimental (solid line) and simulated (filled area) spectra for ^{241}Am point source measurements.

were supposed to be efficiency in counts/s/Bq but, in fact, some participants misunderstood the meaning of counting efficiency or misunderstand the units provided by the Monte Carlo code they used (see Section 3.4 for more details).

The final results for the three requested efficiencies and the P0 and P4 cases are given in Table 6. From the data of Table 6 it was concluded that, for a given energy, participants have obtained about the same agreement in the P0 case as in the P4 case. Participant G who used the PENELOPE code reported that due to difficulties in defining the source the results might lack in precision for the P4 case and indeed he is the only participant whose results are significantly different between the P0 and P4 cases. The results of participant F were not reviewed by the participant but he agreed to apply the correction factor obtained during the analysis of results. Participants F and Q computed the requested spectra but did not use these spectra to calculate the efficiencies that were calculated in a more direct manner by simulating only the photopeak energy. To obtain a synthetic indicator of the agreement between calculation and experiment the average of the absolute value of participants' relative deviation was considered for all efficiencies. As illustrated in the last line of Table 6 the efficiency at 185.7 keV is usually in better agreement than that at 63.3 and 143.8 keV. Taking into account all participants and the P0 and P4 cases, the typical agreement at 185.7 keV was around 3% while it was around 7% for the other energies. These values are typical values that summarise the results but not an exact average performed over all results. At 63.3 keV underestimation of efficiency clearly dominates for the P0 and P4 cases. At 145.8 and 185.7 keV, for the P0 case overestimations of efficiency are more frequent than underestimates, and for the P4 case over- and underestimates are about the same. If calculated efficiencies are used for an activity assessment, an overestimate of efficiency will lead to an underestimate of the retained activity and thus an underestimate of the dose.

A selection of computed spectra is compared with the experimental spectra, from which the background was subtracted, in Fig. 2. All codes reproduce well the relative heights of photopeaks and to a lesser extend the Compton scattering. In the P0 case, the Compton profile is quite well simulated for energies higher than 60 keV, for lower energies the simulation overestimates this component of the spectrum. In the P4 case the disagreement between simulated and experimental Compton components is more important, noticeable disagreements appear for energies below 100 keV, nevertheless the relative heights of main photopeaks are still well described and not too much affected by the height of the Compton components. Depending on the participants, the agreement of simulated and experimental spectra below 100 keV can be better, compare for example participants L and M in Fig. 2. Several reasons can account for these disagreements:

- more or less detailed electron transport can be used;
- uncertainties about the material composition of detectors and photons;
- the shielding of detectors is not simulated;
- small disagreement between the real and simulated volumes of lungs.

The influence of some of these parameters in the simulation has been illustrated in (Ménard, 2004).

All participants managed to implement the provided voxel phantoms in their MC codes without support from the organisers. Fig. 3 illustrates the implemented geometry in the MCBEND software.

3.4. Most frequent cause of errors and recommendation

3.4.1. Ambiguities due to the definition of tasks

In the text sent to participants, the point source activity was not given, thus computation of the experimental count rate and production of the spectrum in units of counts/s was not possible. Hopefully, most of time, participants provided results for a specified

Table 6
Comparison of experimental and simulated counting efficiencies for task 2.

		P0 case			P4 case		
		63.3 keV	143.8 keV	185.7 keV	63.3 keV	143.8 keV	185.7 keV
Experimental efficiency [counts/s/Bq]		3.25×10^{-4}	9.34×10^{-4}	4.220×10^{-3}	1.921×10^{-4}	6.07×10^{-4}	2.79×10^{-3}
Participant ID	Status	Difference with experiment for calculated counting efficiencies ($100 \times$ (calculated − experiment)/experiment); %)					
A	–	–	–	–	–	–	–
B	Corr.	−3.4	−3.7	−1.4	−4.7	−5.0	−1.3
C	Corr.	−6.8	6.4	−2.8	−9.9	3.9	−4.2
D	Acc.	−4.3	−4.0	−0.5	−6.3	−4.0	−2.0
E	Corr.	−13.2	1.0	1.8	−17.8	−0.2	1.2
F	Corr.	3.6	11.5	3.8	2.0	10.3	4.2
G	Acc.	−10.3	−3.2	1.4	11.5	15.5	20.5
H	Acc.	−1.6	20.3	2.8	−1.0	12.8	0.7
I	Corr.	−1.5	17.8	−0.9	0.6	13.8	−2.0
J	Corr.	−1.5	17.8	4.3	−1.1	13.6	4.1
K	Acc.	3.3	13.7	3.6	2.1	13.9	4.2
L	Acc.	0.9	1.2	4.3	−1.1	−6.3	3.0
M	Corr.	−4.3	−1.6	0.9	−6.9	−5.0	−2.2
N	Corr.	−6.0	0.0	5.6	−9.7	−3.7	3.3
O	Corr.	17.3	1.1	4.2	15.7	−7.1	1.3
P	Corr.	−6.9	−0.9	1.9	−10.2	−5.6	0.0
Q	Acc.	−7.9	−0.5	0.4	−13.1	−5.6	−1.3

The status "Acc." means that submitted results did not required corrections ("Corr."). Participant A only took part in task 1.

activity (1 Ci, 1 Bq, the true activity of the source for those who participated in the last exercises), and it was thus possible to compare the provided spectra, as shown in Fig. 1, where a normalisation for a 1 Bq source was applied.

In the text sent to participants the gamma rays of ^{230}Th were included, but since its half-life is 7.7×10^4 years, secular equilibrium with ^{234}U is not reached and it was not necessary to include it in the simulations. Some participants used their own database to simulate the gamma rays to be included, others used the provided data but noticed that ^{230}Th had not to be included, but some have included ^{230}Th, which results in a quite important photopeak at 67.7 keV (see participants I and K in Fig. 2).

Finally, although the counting efficiency was defined, a tutorial should have been given in the text sent to participants in order to homogenise the calculation methods.

3.4.2. Most frequent causes of errors

It is noteworthy that almost all computed spectra scaled with the experimental spectra, i.e. apart from normalisation factors the spectra were correct. This leads to two important conclusions. First, in MC calculations the source term was correctly described, that is to say that the relative importance of gamma rays corresponded to the physical reality and it means that the activities of uranium isotopes and their short-life daughters were correctly taken into account to weigh the gamma rays in the source term. Second, the scaling factor problem reveals difficulties in understanding the units provided by the MC codes. Indeed, the scaling factors identified during the first analysis showed that instead of calculating the spectrum corresponding to 1 s counting for the specified lung activities some participants have calculated:

- the spectrum corresponding to 1 s of counting for a 1 Bq source;
- the spectrum corresponding to 1 s of counting for a source emitting 1 photon/s;
- the spectrum corresponding to 1 s of counting for a source emitting the inverse of the photon emission rate.

Other participants normalised the calculated spectrum by the energy bin width or its inverse; others tried to introduce the number of simulated particles in their normalisation.

When such errors were made the calculated efficiencies are different from the measured one by orders of magnitude. If one has experience in the field of *in vivo* monitoring the calculated values are so different from laboratory practice that the error can be detected. However, the participants were not always directly involved in routine *in vivo* monitoring and thus not familiar with the expected counting efficiencies. It is noteworthy that most of teams involved in routine measurements have directly provided correct results.

3.4.3. Recommendations

The recommendations given here are mostly dedicated for the MCNP or MCNPX codes but are general enough to be extended to other codes.

It is needed to define a discrete probability density function for the energy of emitted gamma rays. For a gamma ray at energy E_i, the emitted photon flux (number of gammas/s) depends on the yield, $y(E_i)$ (number of emitted gamma per nuclear transition) and on the activity, $A(E_i)$ (in Bq):

$$\varphi(E_i) = y(E_i)A(E_i).$$

In the case where several radionuclides have gamma emission at the same energy or at very close energy a sum must be performed over radionuclides. In the case of the simulated experiment, the activity for the daughter radionuclide is the parent's one.

The total photon flux is simply:

$$\varphi = \sum_i \varphi(E_i)$$

and gives the total number of photon emitted by the specified source during 1 s.

To build the probability distribution one simply attributes the probability p_i to the energy E_i with:

$$p_i = \frac{\varphi_i(E_i)}{\varphi}.$$

The probability distribution for enriched uranium has been explicitly given by participant L to explain its calculation and is reproduced here in Table 7 (for readability the sum of probability is normalised to 100). The total photon flux, taking into account the

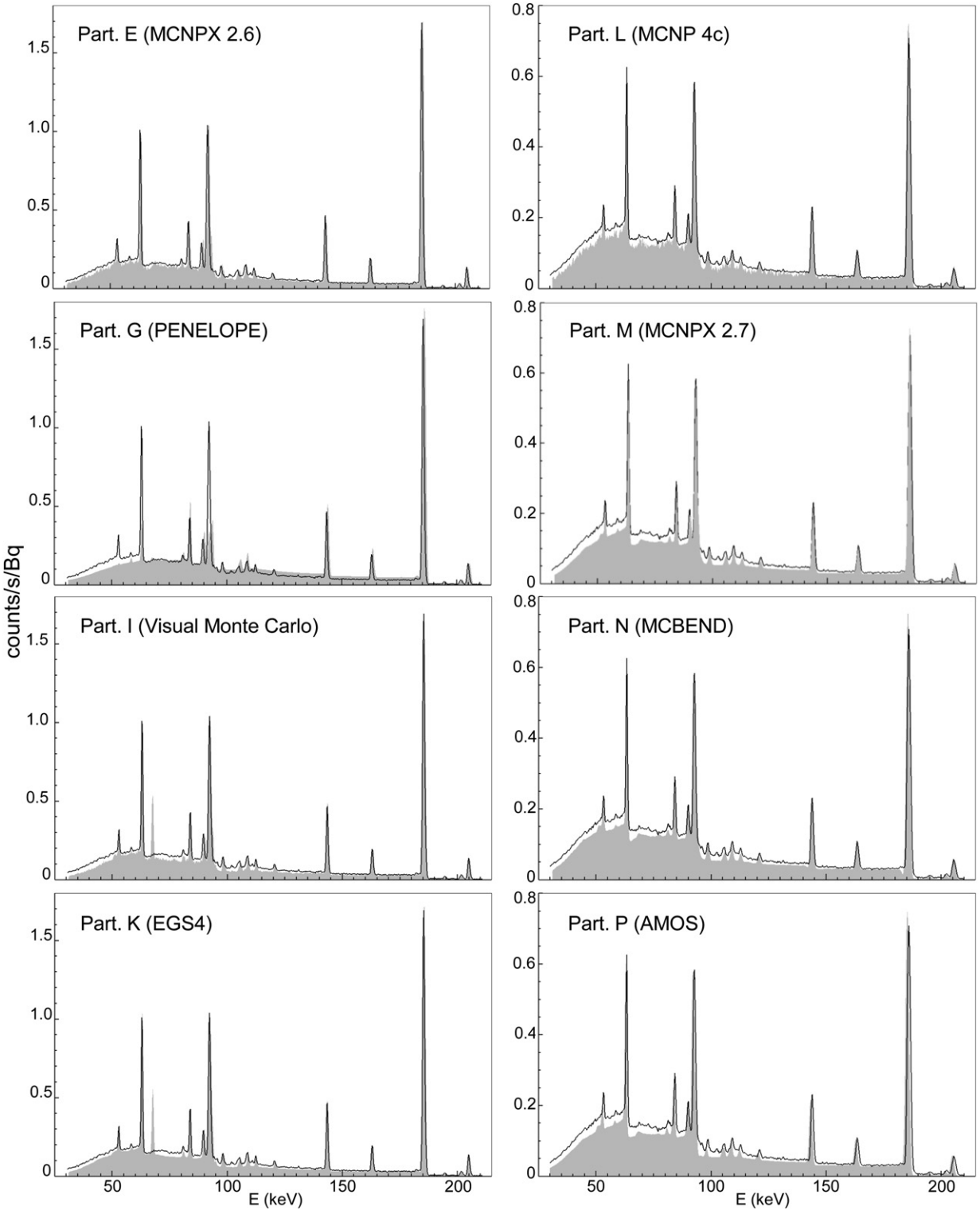

Fig. 2. Comparison of experimental (solid line) and simulated (filled area) spectra for *in vivo* measurements, on left side P0 case, on right side P4 case.

^{234,231}Th and ^{234m}Pa is 2796 gamma/s, it is equivalent to 5.38×10^{-2} photon/s for 1 Bq of enriched uranium, taking into account the three isotopes listed in Table 1.

Once the probabilities for emission have been defined, one needs to normalise the output of the MC calculations to correspond to the requested physical units. Monte Carlo codes normalise their results to one emitted particle so that the result is independent of the number of simulated particles. For a source with only gammas, the MCNPX F8 tally (pulse height tally) gives the number of events in the energy bins for *one* emitted gamma. If the F8 tally is multiplied by φ, the number of events for 1 s is obtained. If one further multiplies by the counting time the number of events during the counting time is simulated.

The definition of a complete source enables to obtain the full spectrum that can be processed like an experimental spectrum to

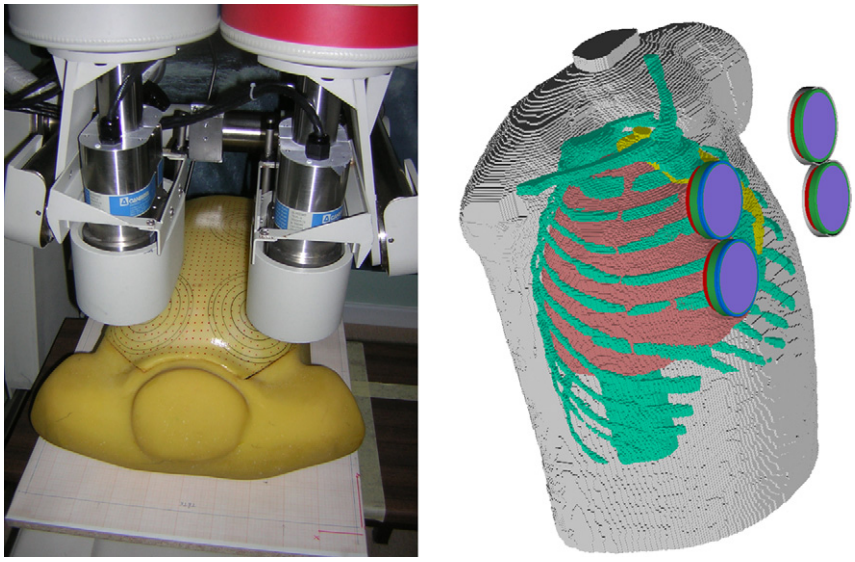

Fig. 3. Picture of the experiment showing the Germanium detectors, the Livermore phantom with the P0 plate and the reference frame to report positions (left), voxel model of the phantom with detectors as provided by the MCBEND/Visual Workshop software (the detector shielding is not simulated).

deduce the counting efficiency at a given energy. However this method might not be the most suitable for efficiency calculation. Indeed, only one energy can be simulated and one thus obtains the number of events in the photopeak for one gamma emitted at the given energy. In MCNPX the number provided by the F8 tally in the energy bin of interest is thus the efficiency in units of counts per emitted gamma. Multiplying this number by the yield of the gamma ray gives the efficiency in units of counts/s/Bq. The advantage of such a method is the simplification of the source definition, the simplification of the output processing and the use of all of the simulated particles at a given energy, which gives a more reliable result than if the same number of particles had been used to simulate several gamma rays. This method meets the experimental practice since during the experimental processing of the spectrum the contribution of the Compton scattering is subtracted. Furthermore, it is not necessary to simulate the energy broadening since in the experiment the region of interest is chosen to take into account the all the counts in the photopeak. Only participants G and Q calculated efficiencies using this method, and despite the spectrum provided by participant G is not satisfactory around 63 keV the calculated efficiency at 63.3 keV is in rather good agreement with experimental values.

Table 7
Recommended source definition for simulation of enriched uranium.

Energy (keV)	Radionuclide	Probability (%)	Energy (keV)	Radionuclide	Probability (%)
90.33	^{235}U	2.06	25.64	^{231}Th (^{235}U)	8.36
93.79	^{235}U	3.33	58.57	^{231}Th (^{235}U)	0.28
96.09	^{235}U	0.05	81.23	^{231}Th (^{235}U)	0.51
105.28	^{235}U	0.38	84.2	^{231}Th (^{235}U)	3.81
106.7	^{235}U	0.74	89.95	^{231}Th (^{235}U)	0.54
109.16	^{235}U	1.08	53.2	^{234}U	1.86
143.76	^{235}U	6.32	120.9	^{234}U	0.6
163.33	^{235}U	2.93	63.29	^{234}Th (^{238}U)	11.9
182.61	^{235}U	0.2	92.38	^{234}Th (^{238}U)	7.9
185.72	^{235}U	32.99	92.8	^{234}Th (^{238}U)	7.79
194.94	^{235}U	0.36	98.4	^{234}Th (^{238}U)	0.69
202.11	^{235}U	0.62	112.81	^{234}Th (^{238}U)	0.67
205.31	^{235}U	2.89	95.06	^{234m}Pa (^{238}U)	0.43
			98.93	^{234m}Pa (^{238}U)	0.69

3.5. Extra work performed by some participants

Only two participants contacted CIEMAT to carry out task 3 and took advantage of their visit to achieve experiments outside the scope of this paper. Participant H conducted task 3 with his own *in vivo* facility and had to carry out the full validation of the counting system modelling. As a result task 3 was not successful and no general conclusion can be given regarding the simulation of counting positions difficult to reproduce with accuracy. Nevertheless some participants performed extra work and provided noteworthy results, which might be presented in future separate communications.

Participant G has explored the advantages and drawbacks of using PENELOPE and Peneasy and MCNPX. When voxel phantoms are used, the default version of Peneasy cannot handle enough different materials, nevertheless with some modifications similar results are obtained than with other codes.

Participant F used home made tools to exchange the lungs of the P0 and P4 voxel phantoms because they did not have exactly the same volumes (see Table 2). Efficiencies calculated with the different voxel lungs were in agreement within 2%.

Participant H decided to benchmark his simulation method thanks to experiments carried out with his detectors. Namely, measurements with a point source and a Livermore phantom were carried out and simulated. As a result, participant H was sure to simulate the requested quantities and his results accepted without corrections.

Participants B and Q investigated the possible effect of the beta spectrum of ^{234m}Pa. It was shown that through Bremsstrahlung photons a signal can be induced in the detector, it results in a small contribution with a peak around 50 keV. At this energy the contribution due to ^{234m}Pa could account at maximum for 5% of the signal. Since only two participants investigated this topic the provided results could not be checked, however if this result was confirmed it could, to some extend, explain the difference between simulated and experimental spectra around 50 keV.

4. Conclusions

The goal of this work was to simulate *in vivo* measurements of enriched uranium in the lungs of a thoracic phantom. Reference

measurements were carried out at the CIEMAT *in vivo* counting facility and then detector models, voxel phantoms and all relevant data needed for the simulation were provided to the participants. All the participants managed to implement voxel phantoms in their Monte Carlo, most of time without difficulty. Although a large number of voxels were used in this problem, no memory management problems were reported.

About half of the participants managed to simulate the spectra and counting efficiencies of the *in vivo* measurements without support from the organisers or only had to apply minor corrections. For other participants the spectra were correct up to a scaling factor that can be explained by misunderstanding of the output units of MC codes, or ambiguities in the directive provided by organisers, or inexperience in the field of *in vivo* counting. After analysis of results and corrections applied by participants, the typical agreement of experimental and counting efficiencies was around 5%.

Since application of routine calibration factors, obtained with physical phantoms, but used for the activity assessment of monitored people can result in uncertainty far larger than 5% it might be interesting in some special cases to use numerical calibration for *in vivo* measurements. However, as shown in this paper, careful benchmarking of the simulation must be performed. Before applying a numerical calibration factor, simple and well-defined experiments should be simulated in order to test the simulation methods.

Voxel phantoms are nowadays used in different fields such as nuclear medicine, radiotherapy and radiological protection. Most of time, they are used to calculate quantities that cannot be measured. However, as far as possible, simple experiments should be designed in order to assess the validity of the simulations, as highlighted in this study where measurements were available.

Acknowledgement

The organisers thank Begoña Pérez López and Juan Francisco Navarro Amaro for efficient and enthusiastic support during the measurements at CIEMAT.

References

Baró, J., Sempau, J., Fernández-Varea, J.M., Salvat, F., 1995. PENELOPE: an algorithm for Monte Carlo simulation of the penetration and energy loss of electrons and positrons in matter. Nuclear Instruments and Methods in Physics Research, Section B 100 (1), 31–46.

Briesmeister, J.F., 1997. MCNP – A general Monte Carlo N-particle Transport Code Version 4B. Oak Ridge National Laboratory Report.

Broggio, D., Janeczko, J., Lamart, S., Blanchardon, E., Borisov, N., Molokanov, A., Yatsenko, V., Franck, D., 2009. New method based on Monte Carlo calculation and voxelized phantoms for realistic internal dosimetry: application to a complex and old actinide contamination. Nuclear Technology 168 (3), 824–831.

Browne, E., Firestone, R.B., 1986. Table of Radioactive Isotopes. Wiley, New York.

Cowan, P., Dobson, G., Wright, G., Cooper, A., 2009. Recent developments to the Monte Carlo code MCBEND. Nuclear Technology 168 (3), 780–784.

de Carlan, L., Aubineau-Lanièce, I., Lemosquet, A., Borissov, N., Jourdain, J.R., Jeanbourquin, D., Le Guen, B., Franck, D., 2003. Application of new imaging and calculation techniques to activity and dose assessment in the case of a 106Ru contaminated wound. Radiation Protection Dosimetry 105 (1–4), 219–223.

Dosisoft, 2010. <http://www.dosisoft.com/english/index.html> (accessed July 2011).

Farah, J., Broggio, D., Franck, D., 2011. Examples of mesh and nurbs modelling for *in vivo* lung counting studies. Radiation Protection Dosimetry 144 (1–4), 344–348.

Franck, D., Laval, L., Borissov, N., Guillierme, P., Bordy, J.M., 2001. Development of voxelised numerical phantoms using MCNP Monte Carlo code: application to *in vivo* measurement. Radioprotection 36 (1), 77–86.

Gabler, D., Henniger, J., Reichelt, U., 2006. AMOS – an effective tool for adjoint Monte Carlo photon transport. Nuclear Instruments and Methods in Physics Research, Section B 251 (2), 326–332.

Gómez-Ros, J.M., de Carlan, L., Franck, D., Gualdrini, G., Lis, M., López, M.A., Moraleda, M., Zankl, M., 2007. Monte Carlo modelling for *in vivo* measurements of americium in a knee voxel phantom: general criteria for an international comparison. Radiation Protection Dosimetry 127 (1-4), 245–248.

Gómez-Ros, J.M., De Carlan, L., Franck, D., Gualdrini, G., Lis, M., López, M.A., Moraleda, M., Zankl, M., 2008a. Analysis of a computational problem involving complex voxel geometries. Radiation Protection Dosimetry 131 (1), 24–27.

Gómez-Ros, J.M., de Carlan, L., Franck, D., Gualdrini, G., Lis, M., López, M.A., Moraleda, M., Zankl, M., Badal, A., Capello, K., Cowan, P., Ferrari, P., Heide, B., Henniger, J., Hooley, V., Hunt, J., Kinase, S., Kramer, G.H., Löhnert, D., Lucas, S., Nuttens, V., Packer, L.W., Reichelt, U., Vrba, T., Sempau, J., Zhang, B., 2008b. Monte Carlo modelling of Germanium detectors for the measurement of low energy photons in internal dosimetry: results of an international comparison. Radiation Measurements 43 (2–6), 510–515.

Griffith, R.V., Dean, P.N., Anderson, A.L., Fisher, J.C., 1978. A tissue-equivalent torso phantom for intercomparison of in-vivo transuranic-nuclide facilities. In: Proceedings of an IAEA Conference on Advances in radiation monitoring. IAEA, Vienna, pp. 493–503. IAEA-SM-229/56.

Hunt, J.G., Dantas, B.M., Lucena, E., 1998. Calibration of an *in vivo* measurement system using a voxel phantom. Radiation Protection Dosimetry 79 (1–4), 425–427.

Hunt, J.G., Malátová, I., Foltánová, S., 1999. Calculation and measurement of calibration factors for bone surface seeking low energy gamma emitters and determination of ^{241}Am activity in a real case of internal contamination. Radiation Protection Dosimetry 82 (3), 215–218.

Hunt, J.G., Dantas, B.M., Lourenço, M.C., Azeredo, A.M.G., 2003. Voxel phantoms and Monte Carlo methods applied to *in vivo* measurements for simultaneous ^{241}Am contamination in four body regions. Radiation Protection Dosimetry 105 (1-4), 549–552.

ICRP, 1983. Radionuclide Transformations – Energy and Intensity of Emissions, ICRP Publication 38. In: Annals of ICRP, 11–13. ICRP.

ICRP, 1997. Individual Monitoring for Internal Exposure of Workers, ICRP Publication 78. In: Annals of ICRP, 27. ICRP. 3–4.

ICRP, 2008. Nuclear Decay Data for Dosimetric Calculations, ICRP Publication 107. In: Annals of ICRP, 38 (3). ICRP.

ICRU, 2003. ICRU Report 69: direct determination of the body content of radionuclides. Journal of the ICRU 3 (1).

Isambert, A., Beaudré, A., Ferreira, I., Lefkopoulos, D., 2007. Quality assurance of a virtual simulation software: application to IMAgo and SIMAgo (ISOgrayTM) (Assurance qualité d'un logiciel de simulation virtuelle: application à IMAgo et SIMAgo (ISOgrayTM)). Cancer/Radiotherapie 11 (4), 178–187.

Kinase, S., Takagi, S., Noguchi, H., Saito, K., 2007. Application of voxel phantoms and Monte Carlo method to whole-body counter calibration. Radiation Protection Dosimetry 125, 189–193.

Kramer, G.H., Hauck, B.M., 2002. Comparison of the 1st, 2nd and 3rd generation Lawrence Livermore National Laboratory Torso phantoms. Radiation Protection Dosimetry 102 (4), 323–332.

Lamart, S., Blanchardon, E., Molokanov, A., Kramer, G.H., Broggio, D., Franck, D., 2009. Study of the influence of radionuclide biokinetics on the efficiency of *in vivo* counting using Monte Carlo simulation. Health Physics 96 (5), 558–567.

Lopez Ponte, M.A., Bravo, T.N., 2000. A low energy Germanium detector system for lung counting at the WBC facility of CIEMAT. Radiation Protection Dosimetry 89 (3–4), 221–227.

Lopez, M.A., Balásházy, I., Bérard, P., Blanchardon, E., Breustedt, B., Broggio, D., Castellani, C.M., Franck, D., Giussani, A., Hurtgen, C., James, A.C., Klein, W., Kramer, G.H., Li, W.B., Marsh, J.W., Malatova, I., Nosske, D., Oeh, U., Pan, G., Puncher, M., Telles, P.T., Schimmelpfeng, J., Vrba, T., 2011. Eurados coordinated action on research, quality assurance and training of internal dose assessments. Radiation Protection Dosimetry 144 (1–4), 349–352.

Malátová, I., Vrba, T., Bečková, V., Pospíšilová, H., 2010. Twelve years of follow up of cases with old ^{241}Am internal contamination. Health Physics 99 (4), 495–502.

Ménard, S., 2004. Summary of the P7 problem: peak efficiencies and pulse height distribution of a photon Ge spectrometer in the energy range below 1 MeV. In: Gualdrini, G., Ferrari, P. (Eds.), Intercomparison on the Usage of Computational Codes in Radiation Dosimetry. ENEA, Italy, pp. 289–303.

Newton, D., White, D.R., 1978. Attenuation of 13–20 keV photons in tissue substitutes and their validity for calibration purposes in the assessment of plutonium in lungs. Health Physics 35 (5), 699–703.

Nelson, W. R., Hirayama, H., Rogers, D.W.O., 1985. The EGS4 Code System. SLAC-265 (1985).

Pelowitz, D., 2005. MCNPX User's Manual. Los Alamos National Laboratory Report, LA-CP-05-0368.

Pierrat, N., 2005. Application des fantômes numériques voxelisés associés au code de Monte Carlo MCNP à la mesure in vivo réaliste des actinides dans les poumons et les plaies contaminées. Thesis, Université Paris XI, Faculté de Médecine Paris-Sud.